1.0

4.5
5.0
5.5

2.8

2.5

3.2

2.2

3.6

1.1

4.0

2.0

1.8

1.25

1.4

1.6

MICROCOPY RESOLUTION TEST CHART
NATIONAL BUREAU OF STANDARDS-1963 A

AFML-TR-78-46

LEVEL

ELECTRON SPECTROSCOPIC STUDIES OF SURFACES AND INTERFACES FOR ADHESIVE BONDING

UNIVERSAL ENERGY SYSTEMS, INC.
JOHN T. GRANT / GERALD E. HAMMER
3195 PLAINFIELD ROAD
DAYTON, OHIO 45432

MAY 1978

TECHNICAL REPORT AFML-TR-78-46
Interim Report for Period January 1977 — January 1978

DDC
RECEIVED
AUG 21 1978
A

AIR FORCE MATERIALS LABORATORY
AIR FORCE WRIGHT AERONAUTICAL LABORATORIES
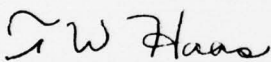AIR FORCE SYSTEMS COMMAND
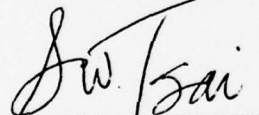WRIGHT-PATTERSON AIR FORCE BASE, OHIO 45433

78
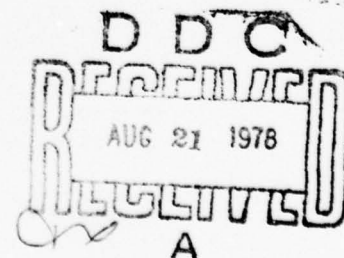
NOTICE

When Government drawings, specifications, or other data are used for any purpose other than in connection with a definitely related Government procurement operation, the United States Government thereby incurs no responsibility nor any obligation whatsoever; and the fact that the Government may have formulated, furnished, or in any way supplied the said drawings, specifications, or other data, is not to be regarded by implication or otherwise as in any manner licensing the holder or any other person or corporation, or conveying any rights or permission to manufacture, use, or sell any patented invention that may be related in any way thereto.

This report has been reviewed by the Information Office (OI) and is releasable to the National Technical Information Service (NTIS). At NTIS, it will be available to the general public, including foreign nations.

This technical report has been reviewed and is approved for publication.
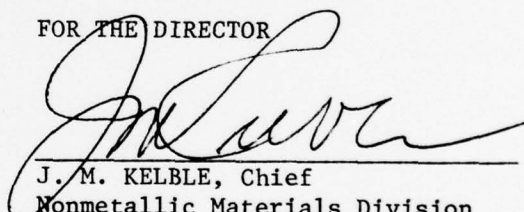
T. W. Haas
Project Engineer

FOR THE DIRECTOR

S. W. Tsai, Chief
Mechanics & Surface Interactions Branch
Nonmetallic Materials Division

FOR THE DIRECTOR

J. M. KELBLE, Chief
Nonmetallic Materials Division

Copies of this report should not be returned unless return is required by security considerations, contractual obligations, or notice on a specific document.

REPORT DOCUMENTATION PAGE		READ INSTRUCTIONS BEFORE COMPLETING FORM
1. REPORT NUMBER AFML-TR-78-46	2. GOVT ACCESSION NO.	3. RECIPIENT'S CATALOG NUMBER
4. TITLE (and Subtitle) ELECTRON SPECTROSCOPIC STUDIES OF SURFACES AND INTERFACES FOR ADHESIVE BONDING		5. TYPE OF REPORT & PERIOD COVERED Interim Report. Jan 77 - Jan 78
		6. PERFORMING ORG. REPORT NUMBER
7. AUTHOR(s) J. T. Grant and G. E. Hammer		8. CONTRACT OR GRANT NUMBER(s) F33615-77-C-5040
9. PERFORMING ORGANIZATION NAME AND ADDRESS Universal Energy Systems, Inc. 3195 Plainfield Road Dayton, Ohio 45432		10. PROGRAM ELEMENT, PROJECT, TASK AREA & WORK UNIT NUMBERS 2303-Q1-02
11. CONTROLLING OFFICE NAME AND ADDRESS Air Force Materials Laboratory (AFML/MBM) Air Force Wright Aeronautical Laboratories Wright-Patterson Air Force Base, Ohio 45433		12. REPORT DATE May 1978
		13. NUMBER OF PAGES 52
14. MONITORING AGENCY NAME & ADDRESS(If different from Controlling Office)		15. SECURITY CLASS. (of this report) Unclassified
		15a. DECLASSIFICATION/DOWNGRADING SCHEDULE

16. DISTRIBUTION STATEMENT (of this Report)

Approved for public release; distribution unlimited

17. DISTRIBUTION STATEMENT (of the abstract entered in Block 20, if different from Report)

18. SUPPLEMENTARY NOTES

19. KEY WORDS (Continue on reverse side if necessary and identify by block number)

Adhesive Bonding
Electron Spectroscopy
X-ray Photoelectron Spectroscopy
Auger Electron Spectroscopy
Surface Analysis

20. ABSTRACT (Continue on reverse side if necessary and identify by block number)

This report describes work carried out in the first twelve months of a twenty eight month contract to study the interaction of simple organic molecules on aluminum and titanium surfaces prepared for adhesive bonding using electron spectroscopic techniques. Other electron spectroscopic studies of specimens related to the surface phenomena program are also reported.

DD FORM 1473   EDITION OF 1 NOV 65 IS OBSOLETE
1 JAN 73

390 743   LB

FOREWORD

This interim report describes the results of a research program in progress to study surfaces and interfaces for adhesive bonding using electron spectroscopy. This report covers the period January 1977 through January 1978 and is being conducted by Universal Energy Systems, Inc., 3195 Plainfield Road, Dayton, Ohio 45432 at the Air Force Materials Laboratory under Contract F33615-77-C-5040, initiated under Task No. 2303Q1. The research was performed by Dr. J. T. Grant and G. E. Hammer with the technical assistance of R. G. Wolfe and J. R. Miller. The Project Engineer for the Air Force was Dr. T. W. Haas, Nonmetallic Materials Division (AFML/MBM). The authors submitted this report in February 1978.

iii

TABLE OF CONTENTS

LIST OF ILLUSTRATIONS

LIST OF ILLUSTRATIONS (continued)

LIST OF TABLES

SECTION I

INTRODUCTION

The use of adhesive bonding in joining both primary and
secondary structural components of aircraft and spacecraft has
many potential advantages such as reduced weight, reduced machining,
material and assembly costs, efficient transfer of loads between
components, a reduction in problems associated with stress corrosion
in and around rivets that lead to fatigue cracking, etc. Further,
missles and spacecraft could hardly exist without the use of
adhesives as, for example, the attachment of ablative heat shields
to metallic substructures can be made only with adhesives. Because
of the many significant advantages of adhesive bonding as a joining
technique there is a definite need to conduct research in this area,
particularly with a view to improved durability, reliability,
reproducibility, and predictability of failure. One extremely
important area for research is the study of the strength of bonding
between the adhesive and the adherend, including long term effects
such as moisture degradation, phase changes in the anodized layer,
and polymer decomposition. The control and predictability of
such effects require an understanding of how organic molecular
functional groups interact with surfaces prepared for adhesive
bonding.

This report describes work carried out in the first twelve
months of a twenty eight month contract to study the intraction of

1

simple organic molecules such as methanol, acetone, formic acid and methylamine on a aluminum and titanium surfaces prepared for adhesive bonding using electron spectroscopic techniques. Studies of the co-adsorption of water vapor will also be made. Results obtained to date using Auger electron spectroscopy (AES) and X-ray photoelectron spectroscopy (XPS) are reported in Section II. A deconvolution program has also been developed for treating XPS data where effects due to electron spectrometer broadening and X-ray line shape can be largely eliminated. This is described in Section III.

Other electron spectroscopic studies of specimens related to the surface phenomena program are reported in Sections IV, V and VI.

SECTION II

ADSORPTION OF SIMPLE ORGANIC MODECULES ON
ANODIZED MATERIALS

In order to study the adsorption and interaction of simple organic molecules on anodized materials, reference XPS spectra of adsorbed, non-decomposed organic molecules are required. A suitable substrate for obtaining such reference spectra is molybdenum disulfide which has no unsatisfied bonds on a perfect cleavage surface and is very inert. Therefore, molecular adsorption can occur on MoS_2 at low temperatures. To carry out this phase of the work a cold stage for cooling specimens was designed and constructed. By cooling with liquid nitrogen, specimen temperatures down to minus 100°C were obtained.

One problem was noted in cleaning the cleaved MoS_2 surfaces. Inert gas sputtering removed surface contaminants (carbon and oxygen), but also selectively sputtered sulfur, resulting in a sulfur deficient molybdenum disulfide. When acetone was adsorbed on this surface only one carbon XPS peak was found indicating that the acetone had decomposed. This problem was resolved by cleaning the cleaved MoS_2 by heating in the ultra high vacuum system. A surface having the calculated composition of MoS_2 was then obtained and molecular adsorption of acetone was achieved. Reference carbon 1s XPS spectra of molecularly adsorbed methanol and acetone are shown in Figure 1 (a) and (b) respectively. Note that the two carbon 1s lines from the acetone have an intensity ratio of 1:2 corresponding to the two valence states of carbon in acetone. A dummy run was carried out to see if any carbon containing background gases in the vacuum system adsorbed on the cooled MoS_2 during analysis - none were observed to

3
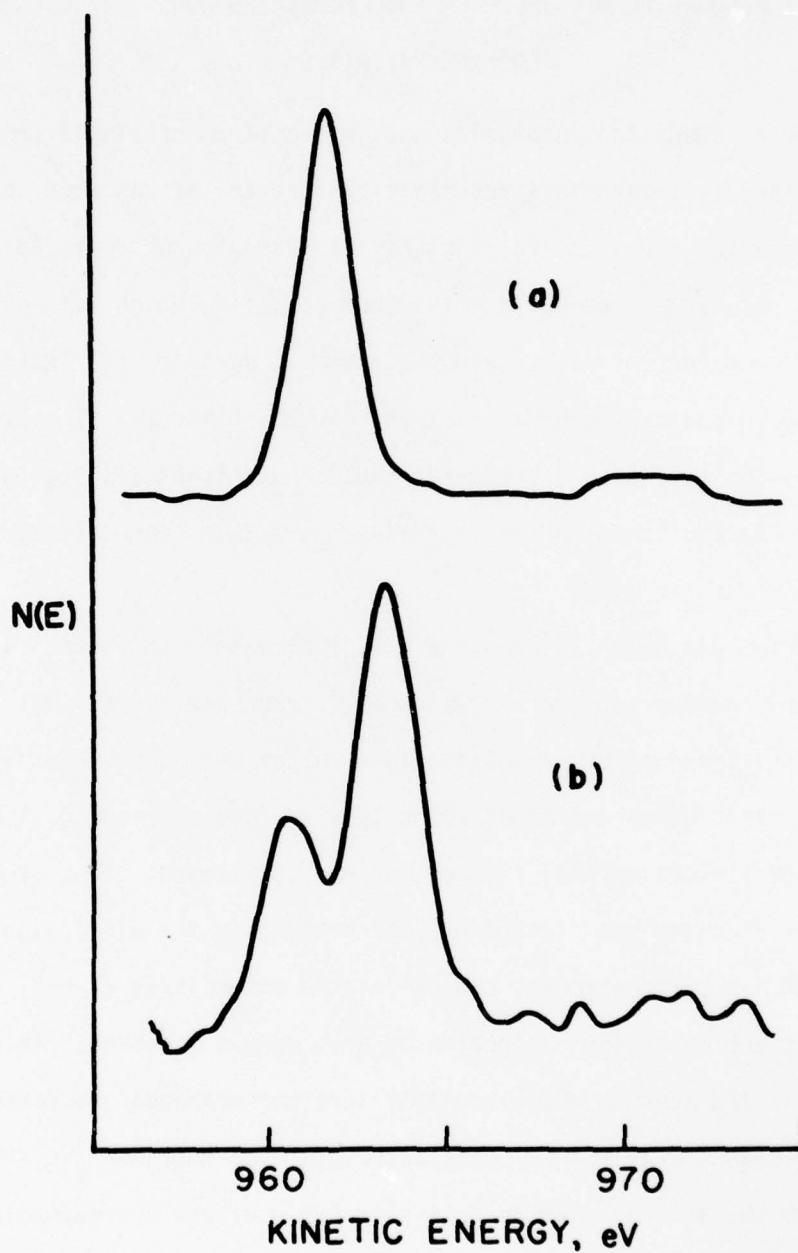
FIGURE 1 - Carbon 1s XPS spectra of molecularly adsorbed (a) methanol and (b) acetone on MoS_2. Spectrometer resolution was 1 eV.

4

adsorb. Cooling MoS_2 to minus 100°C in 5 x 10^{-3} Pa of CO and CO_2
also produced no adsorption (limit of detectability being 2% of a
monolayer).

The first adsorption studies carried out were the adsorption
of methanol on phosphoric acid and chromic acid anodized aluminum.
These two anodization methods were chosen because of the different
corrosion resistances (to water) and different porosities of the
anodized layers - the phosphoric acid anodized specimens have the
better corrosion resistance and larger pores.

1. CHROMIC ACID ANODIZED AL

An XPS spectrum from a chromic acid anodized Al surface is
shown in Figure 2 (a). Note that besides Al and O, C, N, F and Cr
are detected. The chromium comes from the anodization bath, whereas
the N and F remain from the pickling procedure (a mixture of HF and
HNO_3) before anodization. Exposure of this specimen to methanol
at 10^{-4} Pa for 300s (the pressures reported being uncorrected nude
ionization gauge readings) did not show any significant adsorption,
Figure 2 (b). However, after cooling the specimen to minus 100°C
in 10^{-4} Pa of methanol (it takes about 15 min to cool the specimen)
and further exposing it for another 15 min at this temperature,
adsorption did occur as can be seen in the XPS spectrum shown in
Figure 3 (a). Note that the substrate features (e.g. Al) are no
longer detected due to adsorption. The nitrogen peak may arise due

5
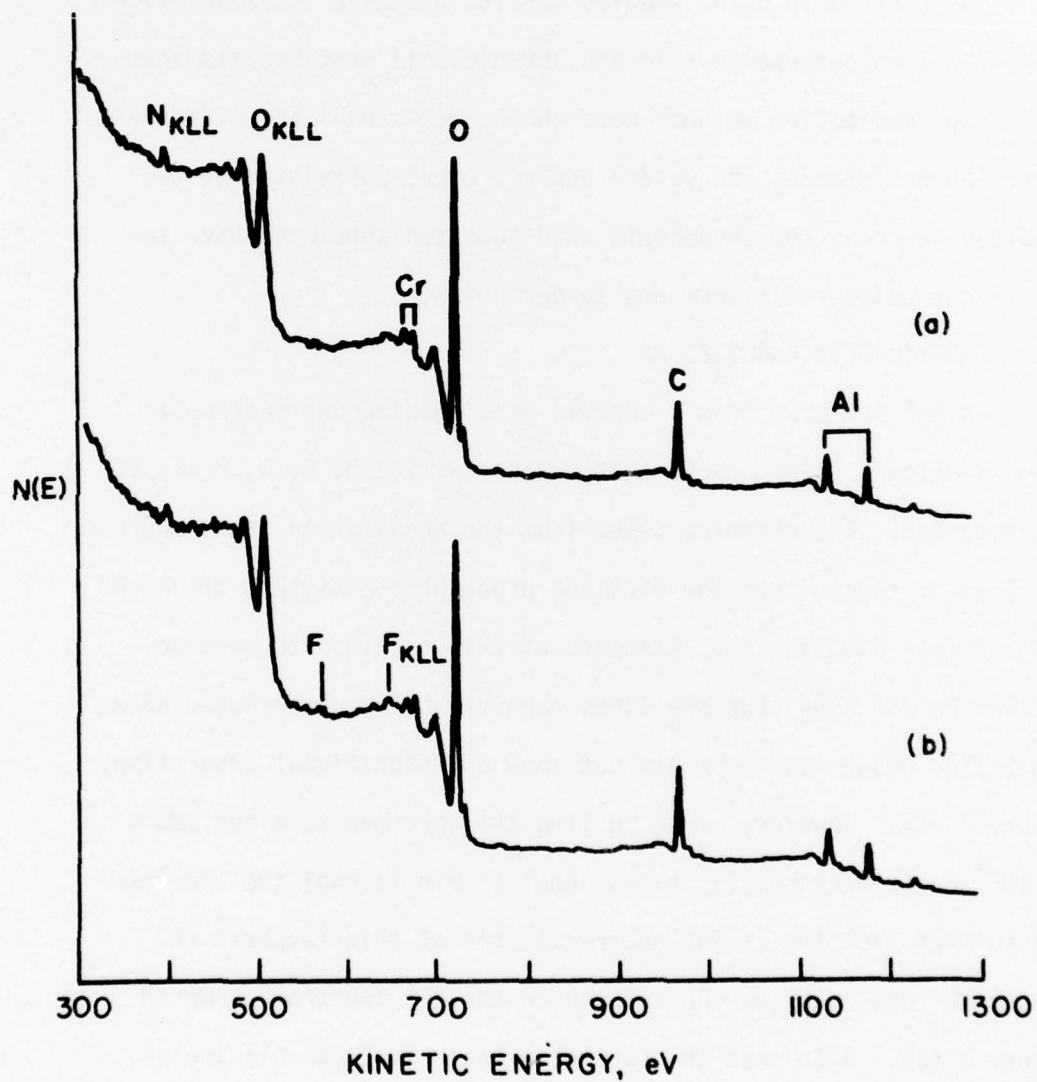
FIGURE 2 - XPS spectra of chromic acid anodized aluminum sur-
face, (a) as prepared, and (b) after exposure to
methanol at room temperature. Spectrometer resolution
was 4 eV.

6
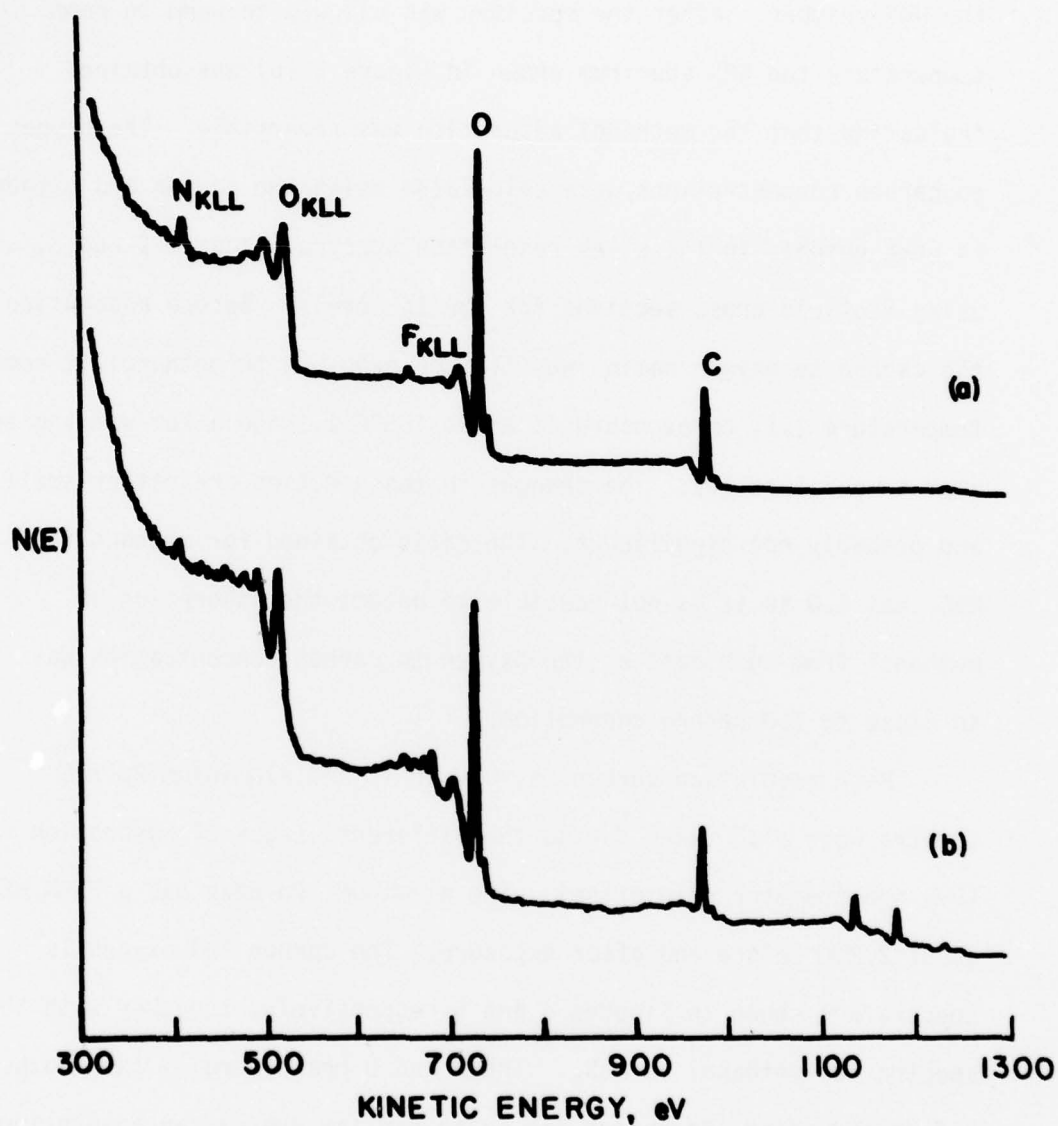
FIGURE 3 - XPS spectra of chormic acid anodized aluminum surface,
(a) after exposure to methanol at minus 100°C, and (b)
after warming to room temperature. Spectrometer reso-
lution was 4 eV.

7

to a small air leak in the cold stage. This spectrum was taken with the specimen held at minus 100°C after evacuating the methanol from the UHV chamber. After the specimen was allowed to warm to room temperature the XPS spectrum shown in Figure 3 (b) was obtained indicating that the methanol adsorption was reversible. The oxygen to carbon concentrations were calculated using the carbon and oxygen 1s peak heights in these 4eV resolution spectra, Figures 2 and 3, and using Scofield[1] cross sections for the 1s levels. Before adsorption the carbon to oxygen ratio was 1.3, on exposure to methanol at room temperature 1.1, on exposure at minus 100°C 1.1, and after warming to room temperature 1.1. The changes in these ratios are rather small and probably not significant. The ratio obtained for methanol on MoS_2 was 1.0 so it is not possible to detect the adsorption of methanol from such data as the oxygen to carbon concentration was so close to 1.0 before adsorption.

High resolution carbon 1s, oxygen 1s and aluminium 2p XPS spectra were also taken during the different stages of adsorption (1 eV spectrometer resolution). The aluminum 2p peak had a FWHM of about 2.2 eV before and after exposure. The carbon and oxygen 1s spectra are shown in Figures 4 and 5 respectively, together with the spectra for methanol on MoS_2. The C and O peak energies and widths before and after adsorption are quite similar whereas an adsorption at minus 100°C the peaks are shifted to higher kinetic energies and the O width was slightly reduced, from 2.8 eV to 2.2 eV. The

8

difference in kinetic energies between the C and O peaks was constant at 245.5 ± 0.3 eV for all the spectra and as the C and O widths on methanol adsorption were larger than the reference spectra it was felt that the specimen was charging electrically for the data shown in Figures 4 (c) and 5 (c). To check for charging another adsorption run was made with the specimen held at minus 100°C and exposed to lower concentrations of methanol. The carbon 1s spectra obtained from the experiment are shown in Figure 6. Here the growth of a new C peak, on the low kinetic energy side of the C peak obtained from the anodized subtrate, is quite apparent with increasing methanol exposure. This C peak is shifted 2.0 eV from the substrate peak and appears at an energy close to that for methanol on MoS_2. This C peak also has a FWHM of about 2.0 eV, close to that for methanol on MoS_2, 1.8 eV. Such problems due to specimen charging often occur in electron spectroscopy and can result in erroneous interpretations if care is not exercized in interpreting data.

2. PHOSPHORIC ACID ANODIZED AL

An XPS spectrum from phosphoric acid anodized Al is shown in Figure 7 (a). Note the presence of phosphorus, due to the anodization bath. Exposure of this specimen to 10^{-4} Pa of methanol for 300s also did not result in any significant adsorption. However, on cooling the specimen to minus 100°C, adsorption did occur and the corresponding XPS spectrum is shown in Figure 7 (b). Again, note the disappearance of the substrate peaks. On allowing the specimen to warm to room temperature the methanol desorbed.

9

FIGURE 4 - Carbon 1s XPS spectra from chromic acid anodized aluminum (a) after cooling in vacuum, (b) following exposure to methanol at room temperature, (c) following exposure to methanol at minus 100°C, (d) after warming to room temperature and (e) methanol on MoS_2. Spectrometer resolution was 1 eV.
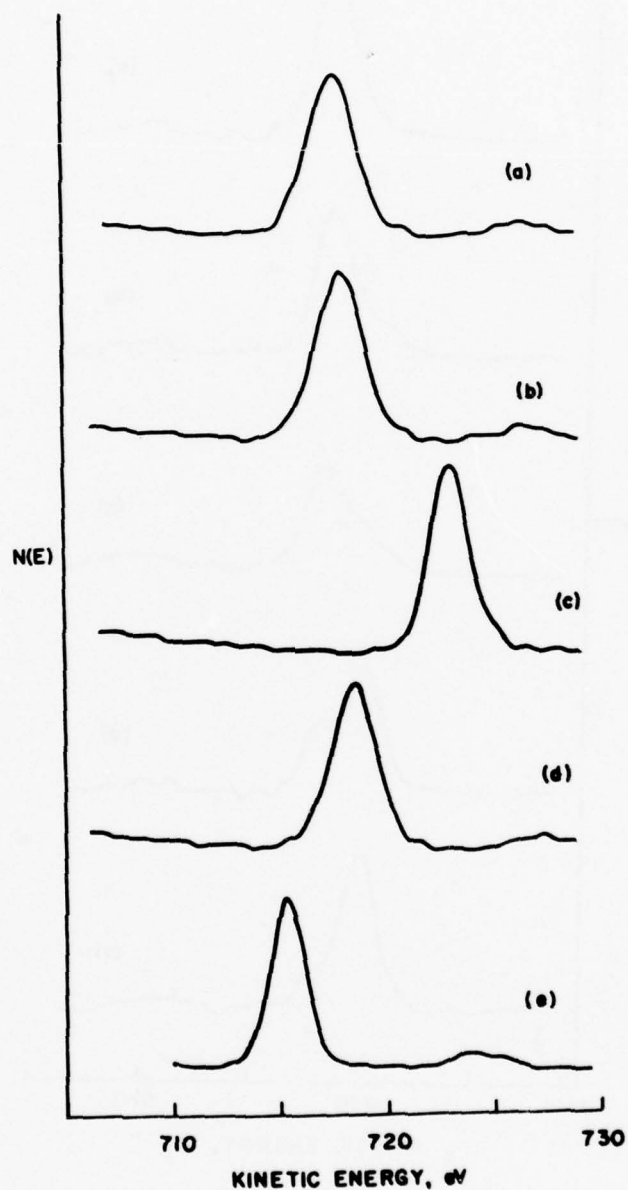
FIGURE 5 - Oxygen 1s XPS spectra from chromic acid anodized aluminum (a) after cooling in vacuum, (b) following exposure to methanol at room temperature, (c) following exposure to methanol at minus 100°C, (d) after warming to room temperature and (e) methanol on MoS_2. Spectrometer resolution was 1 eV.

11
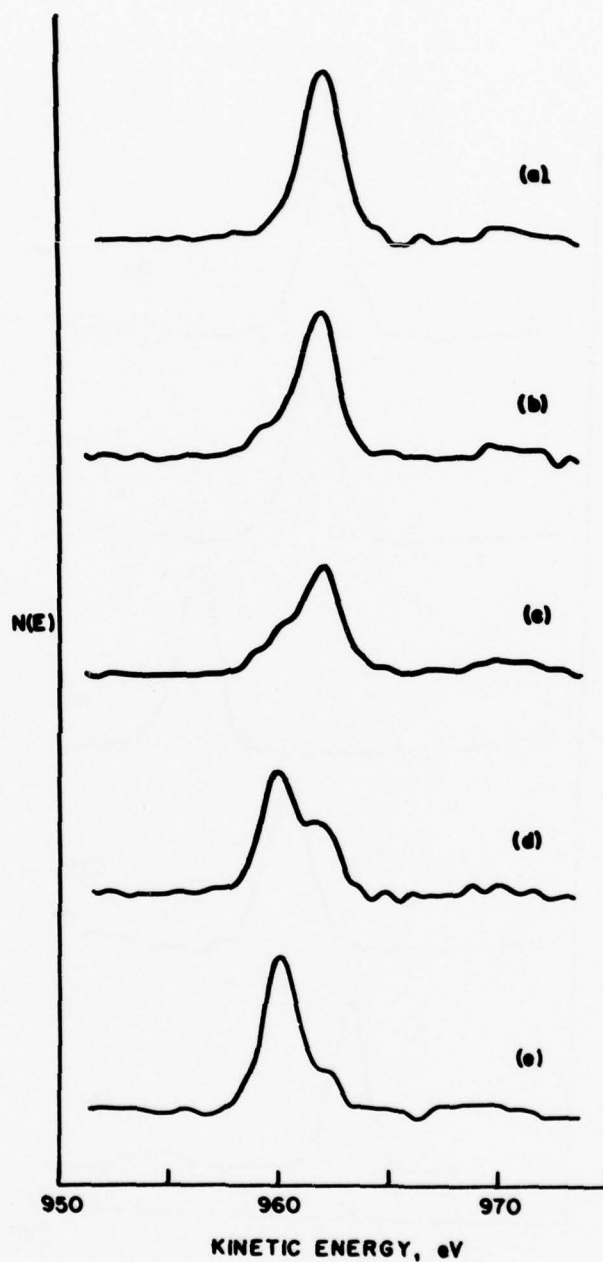
FIGURE 6 - Carbon 1s XPS spectra from chromic acid anodized aluminum (a) after cooling in vacuum, (b) after exposure to methanol at 5×10^{-6} Pa for 2 min, (c) after further exposure to methanol at 1×10^{-5} Pa for 1 min, (d) after further exposure to methanol at 1×10^{-5} Pa for 5 min, and (e) after further exposure to methanol at 1×10^{-5} Pa for 5 min. Spectrometer resolution was 1 eV.

12
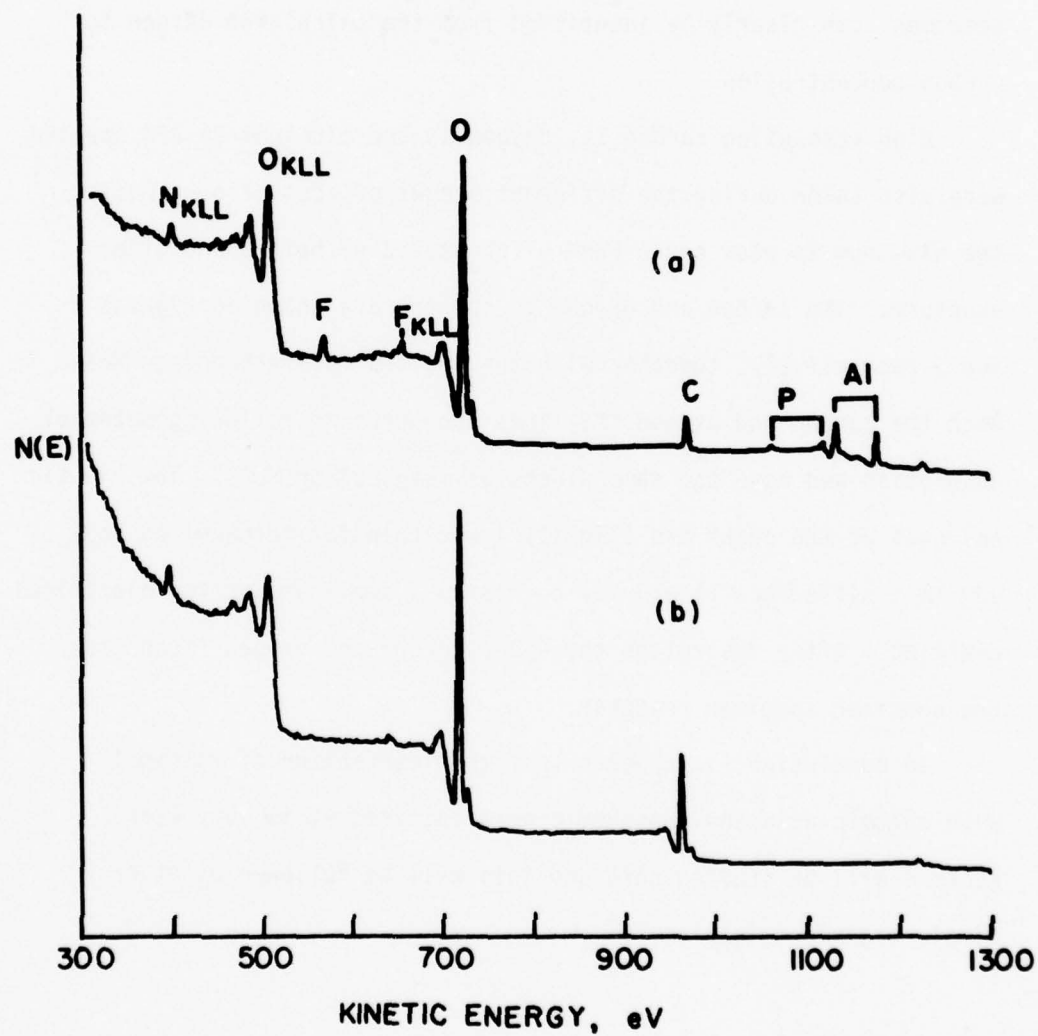
FIGURE 7 - XPS spectra of phosphoric acid anodized aluminum, (a) as prepared, and (b) after exposure to methanol at 10^{-4} Pa for 300s at minus 100°C. Spectrometer resolution was 4 eV.

13

Oxygen to carbon concentrations were also caluclated from these spectra. Before adsorption the carbon to oxygen was 2.7, on exposure to methanol at room temperature 3.4, on exposure at minus 100°C 1.1, and after warming to room temperature 2.9. Unlike the corresponding data for the chromic acid anodized specimen where all ratios were close to unity, the adsorption of methanol on this specimen can clearly be identified from the calculated oxygen to carbon concentration.

High resolution carbon 1s, oxygen 1s and aluminum 2p XPS spectra were also taken during the different stages of adsorption. Again, the aluminum 2p peak had a FWHM of about 2.2 eV before and after exposure. The carbon and oxygen 1s spectra are shown in Figures 8 and 9 respectively, together with the spectra for methanol on MoS_2. Both the carbon and oxygen XPS lines are narrower following methanol adsorption and have the same widths as methanol on MoS_2. The kinetic energies of the peaks are slightly lower than for methanol on MoS_2 and this difference (1 eV) may be due to a small amount for electrical charging. After desorption the wider carbon and oxygen lines from the anodized specimen reappear.

In conclusion, it appears that the interaction of methanol with chromic acid and phosphoric acid anodized Al is very weak. Acetone will be studied next and this will be followed by other simple organic molecules.

14
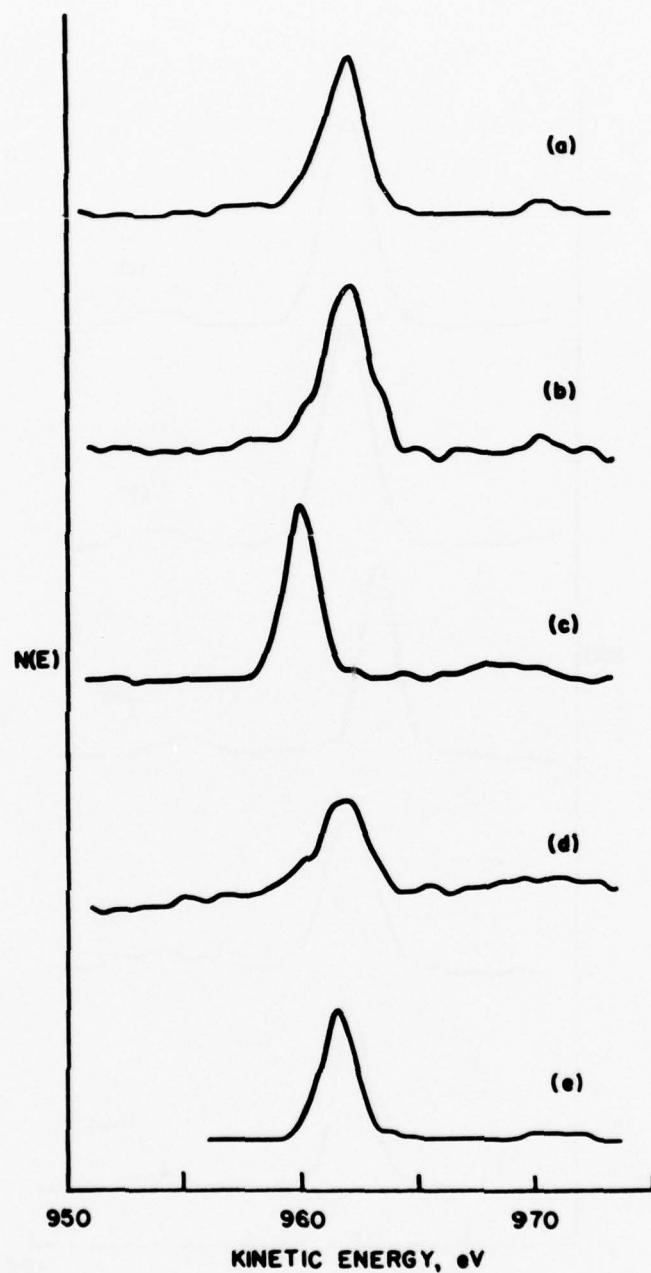
FIGURE 8 - Carbon 1s XPS spectra from phosphoric acid anodized aluminum (a) after cooling in vacuum, (b) following exposure to methanol at room temperature, (c) following exposure to methanol at minus 100°C, (d) after warming to room temperature and (e) methanol on MoS_2. Spectrometer resolution was 1 eV.
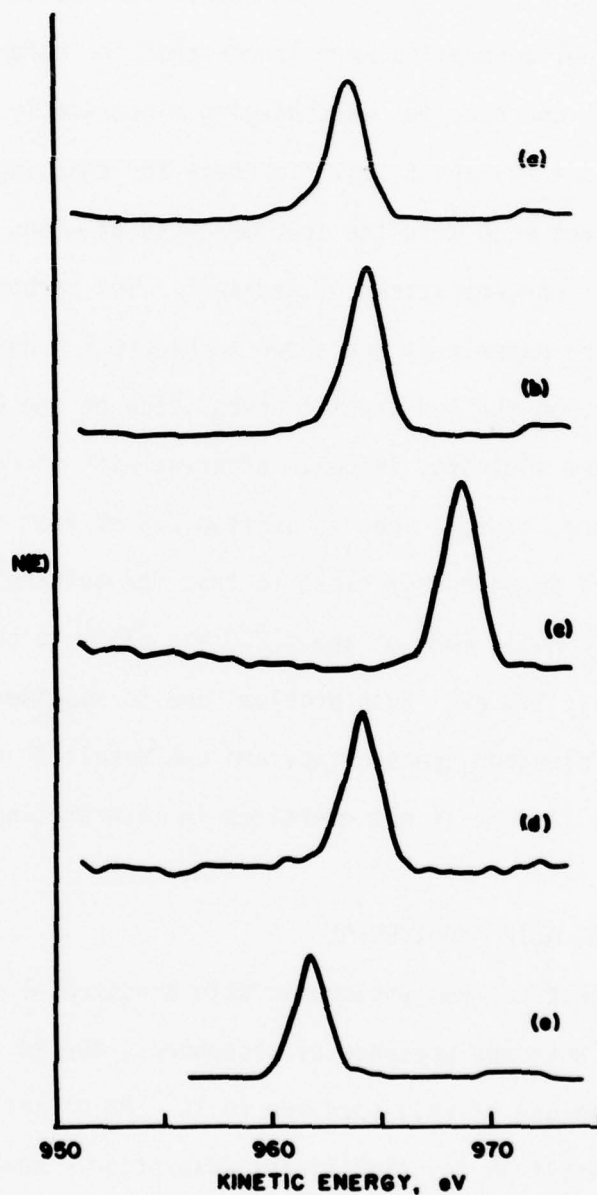
15
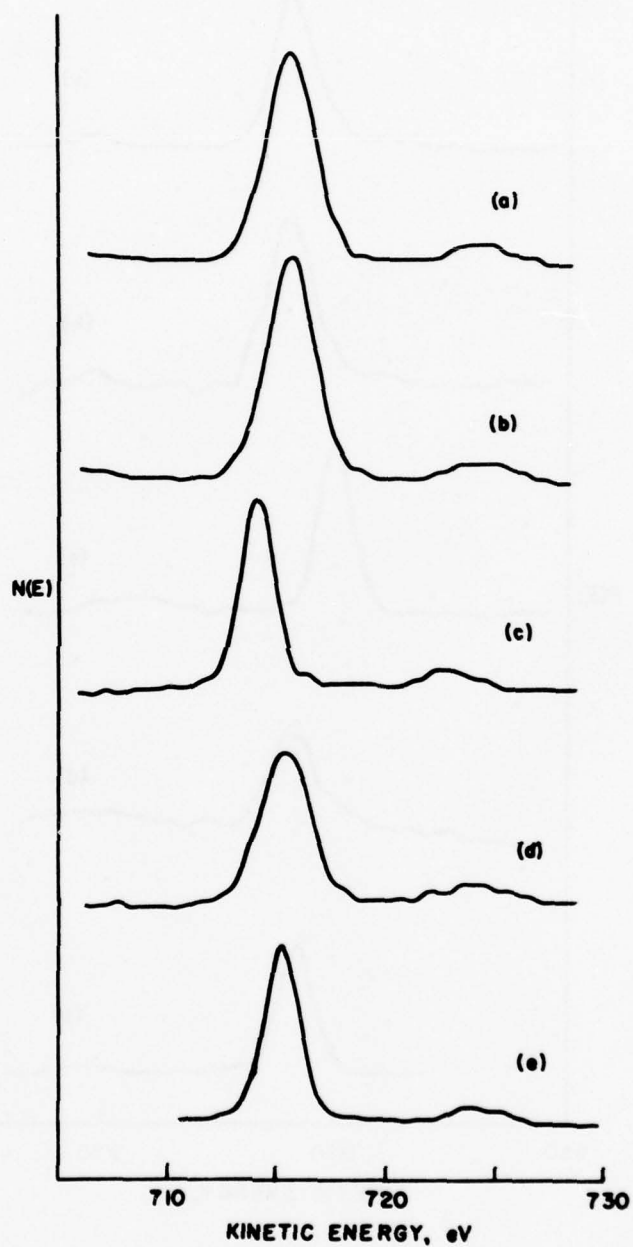
FIGURE 9 - Oxygen 1s XPS spectra from phosphoric acid anodized aluminum, (a) after cooling in vacuum, (b) following exposure to methanol at room temperature, (c) following exposure to methanol at minus 100°C, (d) after warming to room temperature and (e) methanol on MoS_2. Spectrometer resolution was 1 eV.

16

SECTION III

DECONVOLUTION OF XPS SPECTRA

In x-ray photoelectron spectroscopy x-rays emitted from an anode in the x-ray source strike the sample being analyzed, causing photoelectrons to be emitted from the energy levels within the sample. The energies of these electrons are then determined using a cylindrical mirror analyzer (CMA). The characteristics of the resultant spectrum are a combination of those of the anode material, the sample, and the CMA. Therefore, a spectrum as recorded represents the energy levels within the sample, convoluted with the spectral distribution of the x-rays emitted from the anode, and this result convoluted with the response function of the CMA. This convolution process produces a limitation on the information directly available from the spectrum, as it is the binding energies and line shapes and widths of the energy levels in the sample which are useful, and these are somewhat obscured by the spectral distribution of the x-ray source and the response of the analyzer.

Some of the obscured information can be recovered by deconvolution of the data, that is, mathematically processing the data so as to obtain an approximation of one of the components, in this case the energy levels of the sample. If we take F to represent these energy levels, A to represent the response function of the CMA and I to be the energy distribution of the x-rays, the data, H, will be given by the expression

$$H = F*A*I \tag{1}$$

17

where * denotes the convolution operation. The convolution of two functions F and G is defined as

$$F*G = \int_{-\infty}^{+\infty} F(x-y)\, G(y)\, dy = \int_{-\infty}^{+\infty} F(y)\, G(x-y) dy. \tag{2}$$

Note that the operation has the property that

$$F* (G*H) = (F*G)*H = F*G*H \tag{3}$$

that is, it is associative.

We can take the total instrument response function, G, to be

$$G = A*I. \tag{4}$$

The problem then is given the recorded data, $H(E)$, to recover $F(E)$, where

$$H(E) = \int_{-\infty}^{+\infty} F(E-E')\, G(E')\, dE'. \tag{5}$$

If we can determine approximations to the source and analyzer response functions, and therefore $G(E)$, two iterative solutions for $F(E)$ can be found. They are

$$F_0(E) = H(E)$$
$$F_{n+1} = F_n + (H - F_n*G) \tag{6}$$

and

$$F_0(E) = H(E)$$
$$F_{n+1} = F_n \cdot \frac{H}{(G*F_n)} \tag{7}$$

where F_n is the nth approximation to $F(E)$, the approximation improving with increasing n.

In our calculations the approach indicated in equation (7) has been used, for two reasons. First, the negative values often produced in the other method cause the appearance of oscillations of the baseline in the vicinity of the peak. Secondly, it has been observed that the method of equation (7) produces a slightly greater degree of deconvolution for the same number of approximations.[2]

In our XPS studies we have used a double-pass CMA in the retarding mode. This allows us to assume a response function of fixed energy width which is determined by the mirror voltage. Voltages corresponding to full width at half maximum of 1 eV and 4 eV were used. The response of the analyzer was assumed to be gaussian with the appropriate width. The energy distribution of the incident radiation, the Mg K_α lines, was taken from the literature.[3] The convolution of these two functions was calculated numerically, and the result was used as the instrument response function. The deconvolution calculation was then calculated numerically in a computer program (see Appendix).

An initial test of this deconvolution method was performed by comparing a deconvoluted low resolution spectrum with a higher resolution spectrum of the same peaks. A spectrum of the calcium 2p doublet was recorded at 4 eV and at 1 eV resolution. These are shown in Figures 10 (a) and (d), respectively. An instrument response function representing only the broadening caused by the analyzer at 4 eV FWHM was then calculated and a total of 10 deconvolution approximations were made. The spectrum after 4 calculations is shown in Figure 10 (b). Here the

19
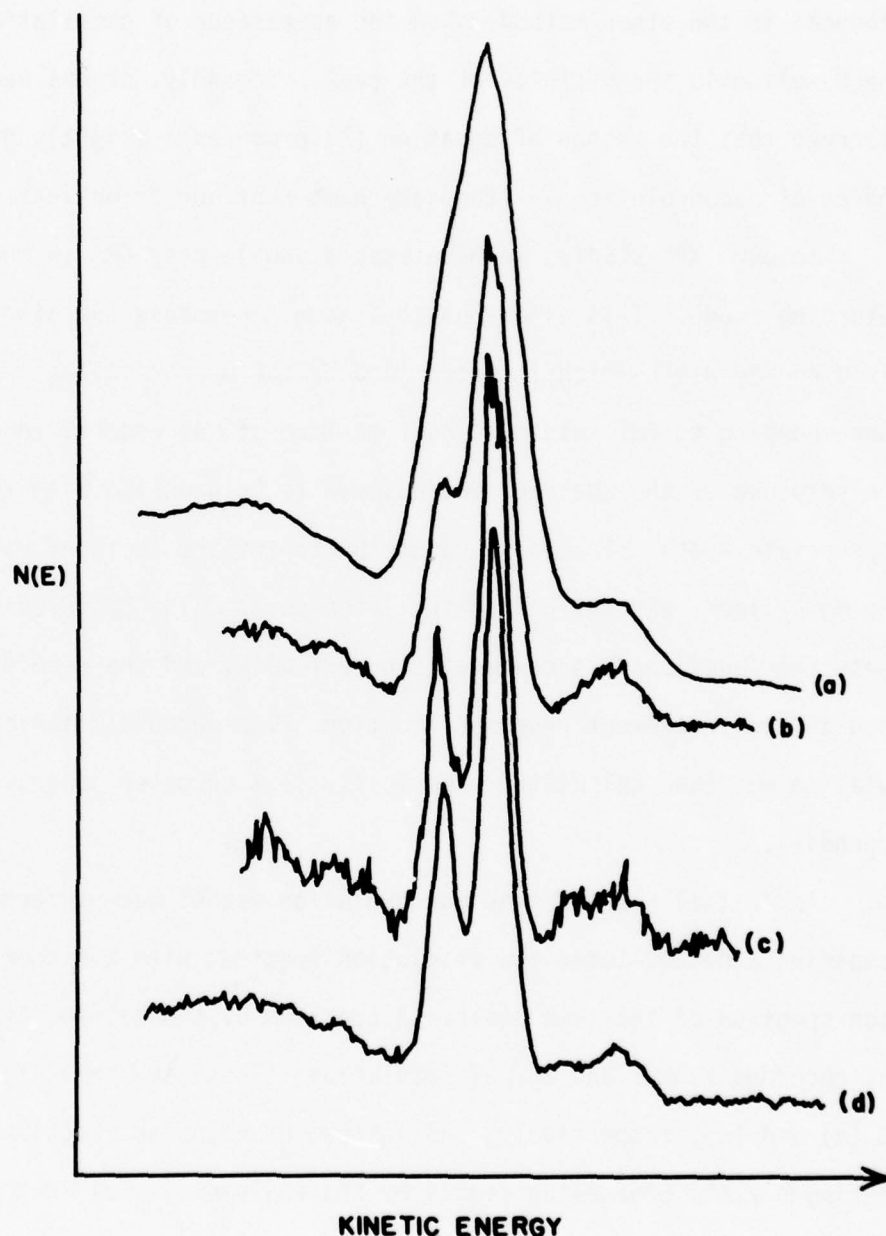
FIGURE 10 - Calcium 2p XPS spectra, (a) raw data with a spectro-
meter resolution of 4 eV, (b) after 4 deconvolution
approximations, (c) after 10 deconvolution approxi-
mations, and (d) raw data with a spectrometer
resolution of 1 eV.

separation of the $2p_{1/2}$ and $2p_{3/2}$ peaks is just appearing. The result after 10 calculations is shown in Figure 10 (c). Here we have achieved a resolution approximately the same as that in the spectrum taken at 1 eV resolution, Figure 10 (d).

A further test of this deconvolution method was made by resolving the Cl_{2p} doublet, which is not resolvable by the XPS system used in this work. A response function including the spectrometer response at 1 eV FWHM and the x-ray line shape for MgK_{α} radiation was used to deconvolute the spectrum shown in Figure 11 (a). The result after 5 approximations is shown in Figure 11 (b). Although the noise is considerably larger, the resolution of the $2p_{1/2}$ and $2p_{3/2}$ peaks is clear. Also note the attenuation of the higher-energy satellite peaks, which is due to the inclusion of the $MgK_{\alpha_{3,4}}$ lines, which produce these satellites, in the x-ray line shape function.

We can conclude that this deconvolution technique can be very useful in recovering information about the energy levels in the samples being analyzed which has been obscured due to instrumental broadening. We must note that, as in the examples above, the signal to noise is considerably reduced by the deconvolution process, so that it requires relatively noise-free spectra as a starting point.
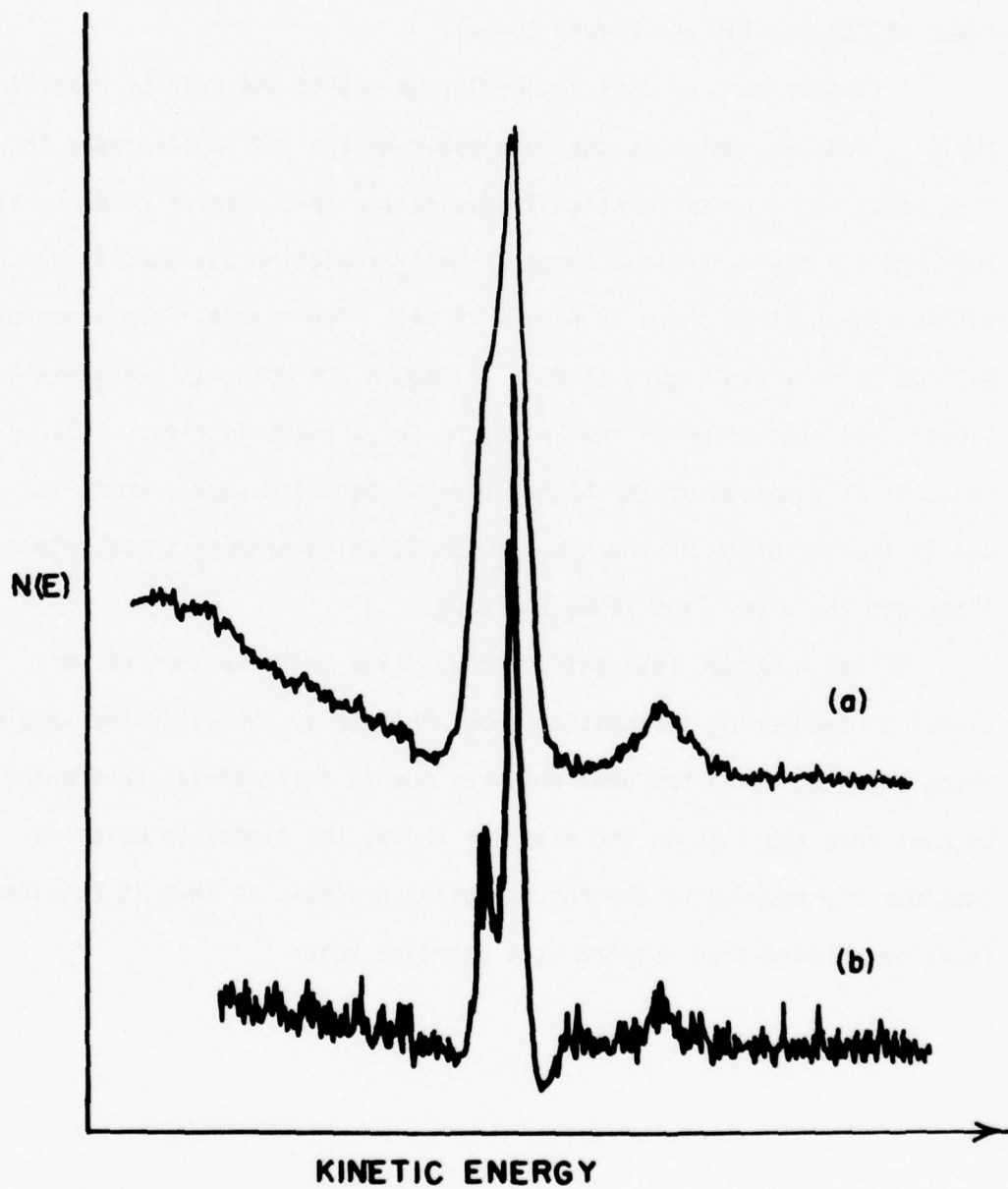
FIGURE 11 - Chlorine 2p XPS spectra, (a) raw data with a spectro-
meter resolution of 1 eV, and (b) after 5 deconvolut-
tion approximations.

SECTION IV

GRAPHITE FIBERS

A number of graphite fibers have been studied during the course of this contract. These fibers were manufactured by Hercules and were prepared by coagulating acrylonitrile polymer in sodium sulfate and then graphitizing at 1500°C for AS and AU type fibers and at about 2000°C for HMS and HMU type fibers. The AS and HMS type fibers were surface treated (oxidized) whereas the AU and HMU type fibers were untreated.

1. COMPARISON OF AS AND AU FIBERS

X-ray photoelectron spectroscopy (XPS) measurements showed that the surface compositions of these fibers were quite different from each other. Typical photoelectron spectra over a kinetic energy range from 100 eV to 1100 eV are shown in Figure 12. Clearly the surface concentrations of oxygen and nitrogen are higher on the AS fibers, Figure 12 (b), than on the AU fibers, Figure 12 (a). Conversely, the surface concentration of sodium is lower on the AS fibers than on the AU fibers.

The larger oxygen concentration on the AS fibers is not unexpected as these fibers have been oxidized. The source of the nitrogen is not certain but its presence could indicate that the fibers were oxidized in nitric acid. The sodium contamination is probably due to coagulation in sodium sulfate.

The carbon, sodium, oxygen and nitrogen 1s photoelectron peak energies and full widths at half maximum (FWHM) were measured at a spectrometer resolution of 1 eV. The carbon, oxygen and sodium peak energies agreed within 1 eV for the four sets of fibers studied. The peak widths

23
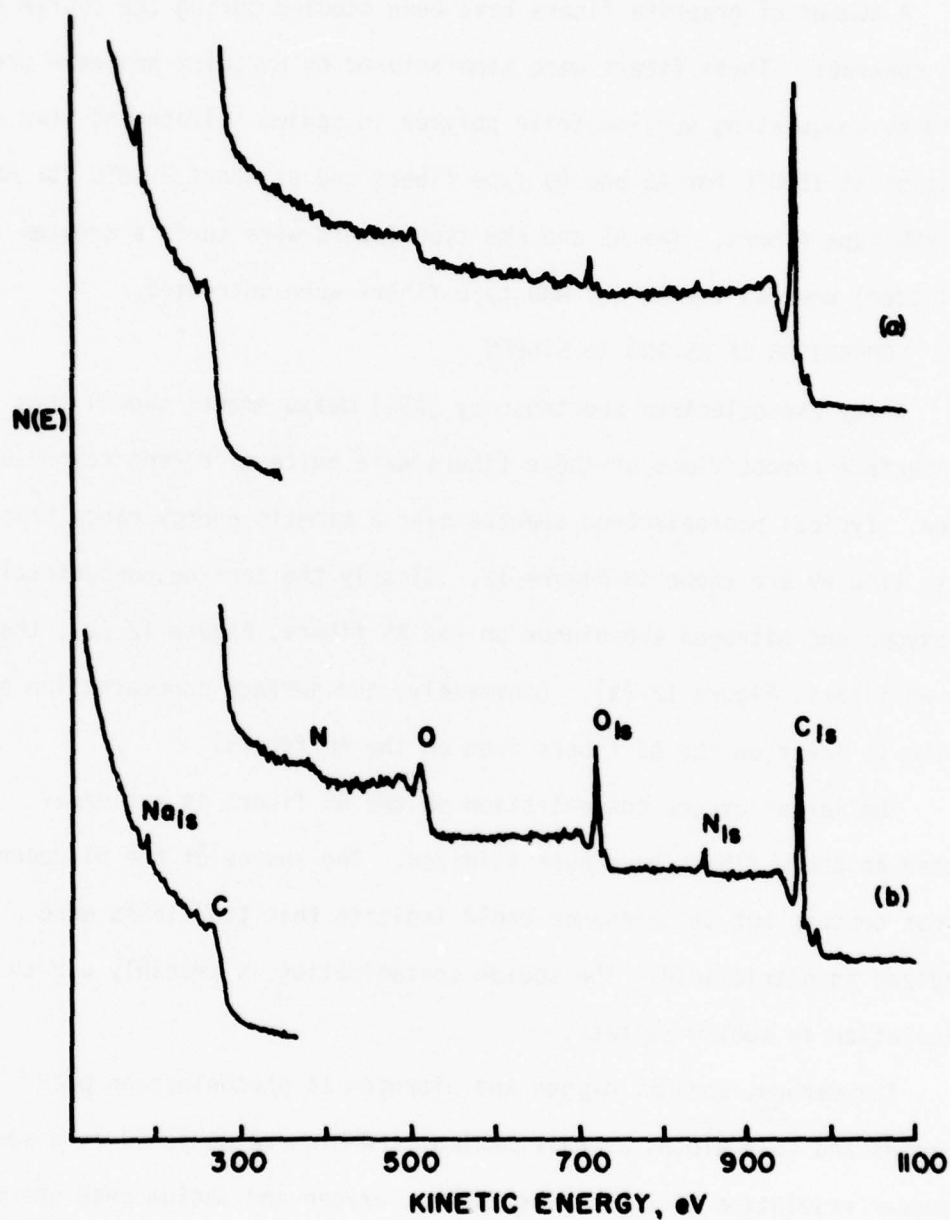
FIGURE 12 - XPS spectra of graphite fibers, (a) AU type fibers, and (b) AS type fibers. Spectrometer resolution was 4 eV.

24

are listed in Table 1. There appeared to be a small carbon peak at about 4 eV higher binding energy than the main carbon peak on the AS fibers. The oxygen peak is wider than expected and may be comprised of more than a single peak. Higher resolution measurements are not feasible in our XPS system due to relatively low count rates. Measurements made on AS fibers using a new XPS system (PHI model 550), having a count rate estimated to be about 15X that used here, at about 0.3 eV spectrometer resolution showed a small improvement in resolution of the measured carbon 1s peak (1.9 eV FWHM) and verified the existence of the small carbon peak at about 4 eV higher binding energy. (With the PHI model 550 at a spectrometer resolution of 0.3 eV the measured FWHM of the silver $3d_{5/2}$ peak is 0.9 eV).

Calculations have been made of the surface concentrations of oxygen, nitrogen and sodium from the XPS data assuming that they are uniformly distributed throughout the surface region. Cross sections were taken from the data of Scofield,[1] and the results are listed in Tables 2 and 3.

It can be seen from these Tables that the sodium concentration for the AU type fibers is about twice that for the AS type fibers. As the sodium 2s XPS peaks can also be measured a check can be made of the uniformity of the sodium distribution throughout the surface layer as the 2s photoelectrons have a kinetic energy of about 1190 eV, compared with about 180 eV for the sodium 1s photoelectrons, and therefore a longer escape depth. (The 2s photoelectrons would have an escape depth about 2½X that of the 1s photoelectrons). For a uniform sodium

TABLE 1

MEASURED FULL WIDTHS AT HALF MAXIMUM (FWHM)
FOR C,O,Na AND N 1s PHOTOELECTRON PEAKS FROM
AS AND AU FIBERS.

		FWHM
Peak	AS Fiber	AU Fiber
C	2.25	2.25
O	3.25	3.25
Na	2.25	2.25
N	2.75	--

TABLE 2

CONCENTRATION IN ATOMIC PER CENT IN GRAPHITE FIBERS:
CALCULATED FROM 1s PEAK HEIGHTS UNDER 4eV RESOLUTION

	$\underline{C}$	$\underline{O}$	$\underline{N}$	$\underline{Na}$
AU_1	88	6.1	-	5.3
AU_2	91	2.7	1	5.3
AS_3	79	15	3	2.8
AS_4	77	15	5.4	2.4
HMU_1	97	2.5	-	-
HMU_2	97	3.1	-	-
HMS_1	94	5.5	-	-
HMS_2	95	4.9	-	-

TABLE 3

CONCENTRATIONS IN ATOMIC PER CENT IN GRAPHITE FIBERS:
CALCULATED FROM 1s PEAK AREAS UNDER 1 eV RESOLUTION -

	$\underline{C}$	$\underline{O}$	$\underline{N}$	$\underline{Na}$
AU_2	92	5.5	-	4.0
AS_4	73	19	5.5	2.4
HMU_2	90	10	-	-
HMS_2	87	13	-	-

27

distribution the ratio of the 1s to 2s peaks should be constant. Measurements on two sets of AU type fibers yielded signal ratios (peak areas not corrected for cross sections or instrument resolution) of 4.17 and 3.72, whereas for AS fibers ratios of 2.04 and 1.84 were obtained. Therefore, it appears that there is a higher concentration of sodium nearer the surface for the AU fibers compared with the AS fibers.

2. COMPARISON OF HMS AND HMU FIBERS

XPS measurements showed that the surface compositions of these fibers were different from each other and from the AS and AU type fibers, Figure 13.

No sodium was detected from the HMS or HMU fibers. As mentioned earlier these fibers were graphitized at a higher temperature than the AS and AU fibers (about 2000°C) so no sodium contamination was expected.

The surface treated fibers, HMS, also showed a larger concentration of oxygen than the untreated fibers, HMU - see Tables 2 and 3.

The carbon and oxygen 1s photoelectron peak energies and full widths at half maximum were also measured at a spectrometer resolution of 1 eV. The carbon and oxygen peak energies from the different fibers were within 0.2 eV for carbon and 0.5 eV for oxygen. The FWHM for carbon and oxygen were measured to be 1.6 eV and 3.4 eV respectively. The FWHM for oxygen is similar to that from the AS and AU fibers, but the FWHM for carbon is considerably narrower than that from the AS and AU fibers (1.6 eV compared to 2.25 eV), Figure 14. This result is not unreasonable as the higher graphitization temperature for the HMS and HMU fibers should result in more truly graphitic surfaces.

28
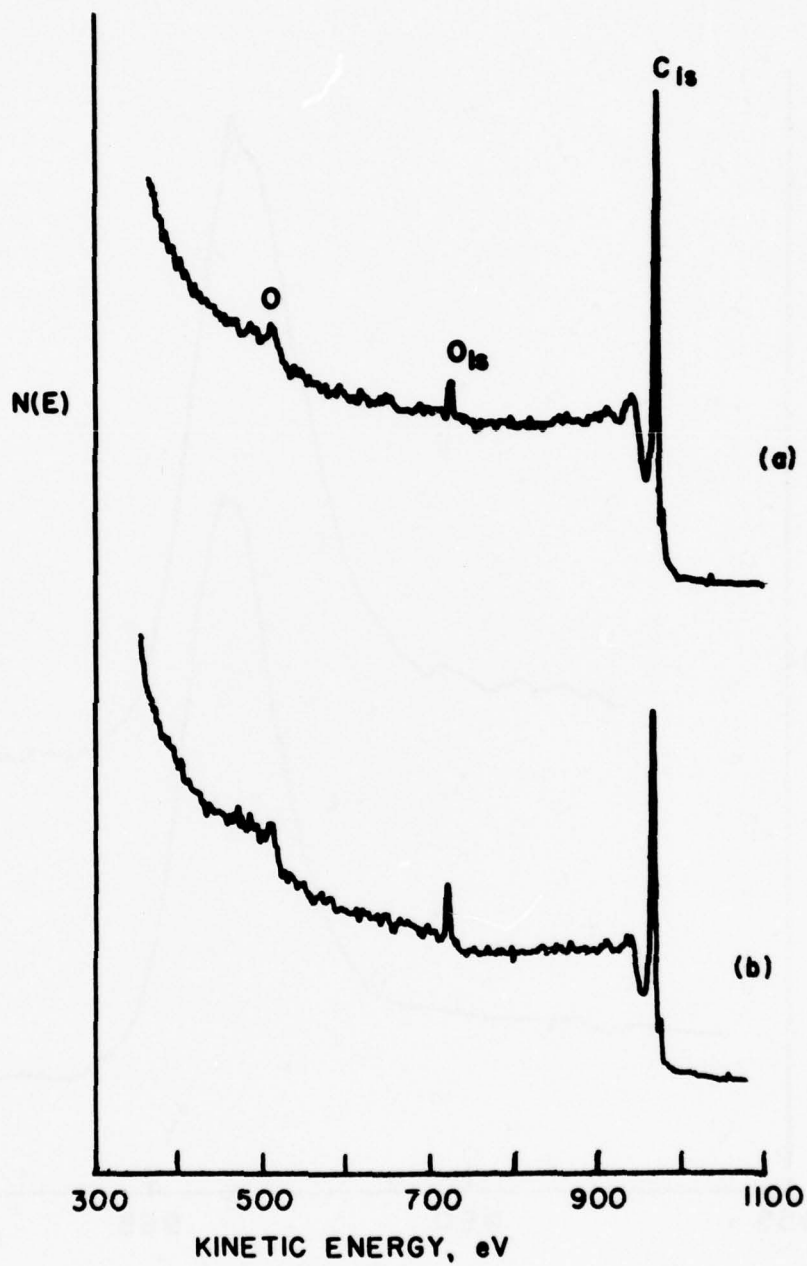
FIGURE 13 - XPS spectra of graphite fibers, (a) HMU type fibers,
and (b) HMS type fibers. Spectrometer resolution
was 4 eV.

29
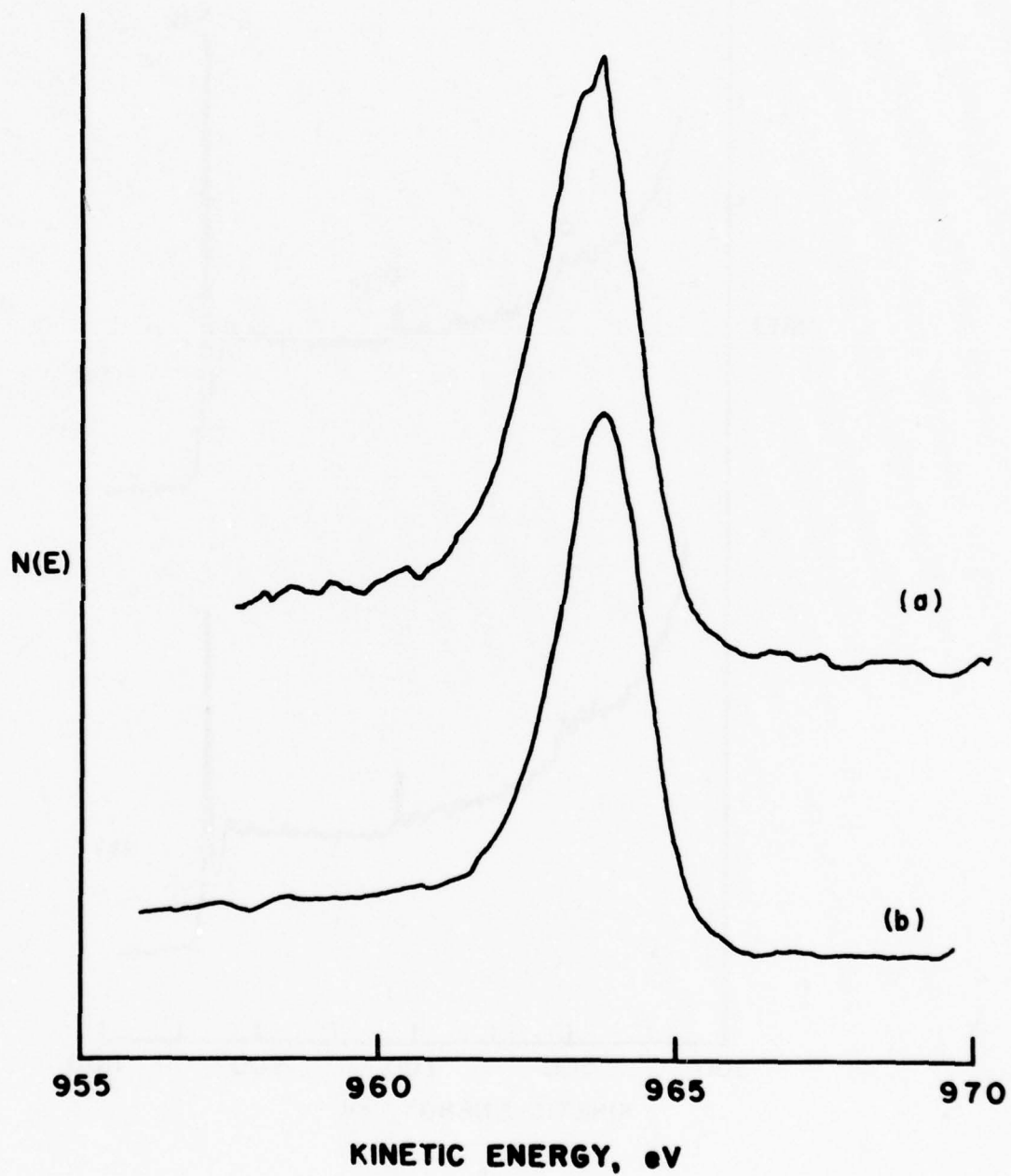
FIGURE 14 - Carbon 1s XPS spectra from, (a) AS type fibers, and
(b) from HMU type fibers. Spectrometer resolution
was 1 eV.

3. FOREIGN MADE FIBERS

A set of foreign made fibers were characterized using Auger electron spectroscopy (AES). Boron, nitrogen, carbon and a small amount of oxygen were detected, Figure 15. The boron and nitrogen Auger line shapes and relative signal strengths indicated the presence of boron nitride (by comparison with a standard spectrum of boron nitride). The boron nitride layer was estimated as approximately 10 nm thick (based on Ta_2O_5 sputtering rate).

FIGURE 15 - Auger electron spectrum from foreign made fibers. Electron beam energy was 3 keV, time constant 0.3s and modulation (sinusoidal) 6 eV peak-to-peak.

32

SECTION V

SOLID LUBRICANT FILMS

Molybdenum disulfide is often used as a solid lubricant film but little is known about changes in chemistry of the film surface that occur during wear. Two partly worn gas bearings were characterized here using mainly XPS. The lubricant film consisted of a mixture of co-sputtered molybdenum disulfide MoS_2 and antimony oxide Sb_2O_3.

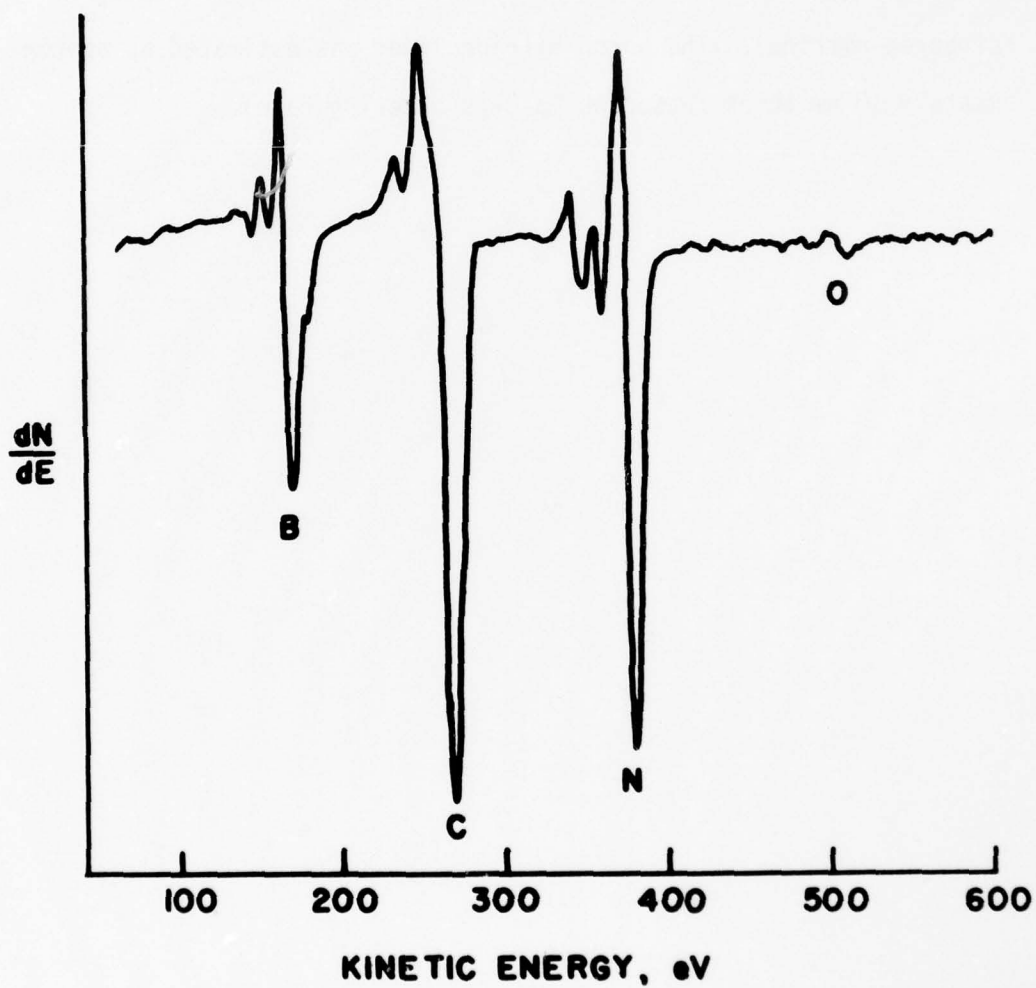AES and XPS survey scans from one of the specimens are shown in Figure 16. The AES spectrum, Figure 16(a), shows the presence of Mo, S, Sb, O(and C). The XPS spectrum, Figure 16(b), also shows the presence of Mo, S, Sb, O (and C) but the oxygen 1s photoelectron peak appeared to overlap the antimony $3d_{5/2}$ peak. This overlap problem was verified by comparing high resolution XPS data from a MoS_2 + Sb_2O_3 burnished film with XPS data from partly oxidized Sb from InSb. These high resolution XPS spectra are shown in Figure 17(a) and 17(b) respectively. In Figure 17(b) two sets of antimony 3d peaks are seen, the more intense pair being from Sb bonded in InSb and the weaker pair being from oxidized Sb. The energies of this latter pair of peaks agree well with those obtained from the burnished film, Figure 17(a). The ratio of the antimony $3d_{5/2}$ to $3d_{3/2}$ peaks was measured to be 1.4 in the oxygen free state whereas it was about 1.8 in the oxidized state and in the burnished film. Obviously the increase in this ratio is due to the overlap of the oxygen 1s peak with the oxidized antimony $3d_{5/2}$ peak.

Useful information about the oxidation of molybdenum sulfide has also been obtained using XPS. Molybdenum 3d spectra from two partly worn gas bearings are shown in Figure 18. Like antimony, the molybdenum 3d

33

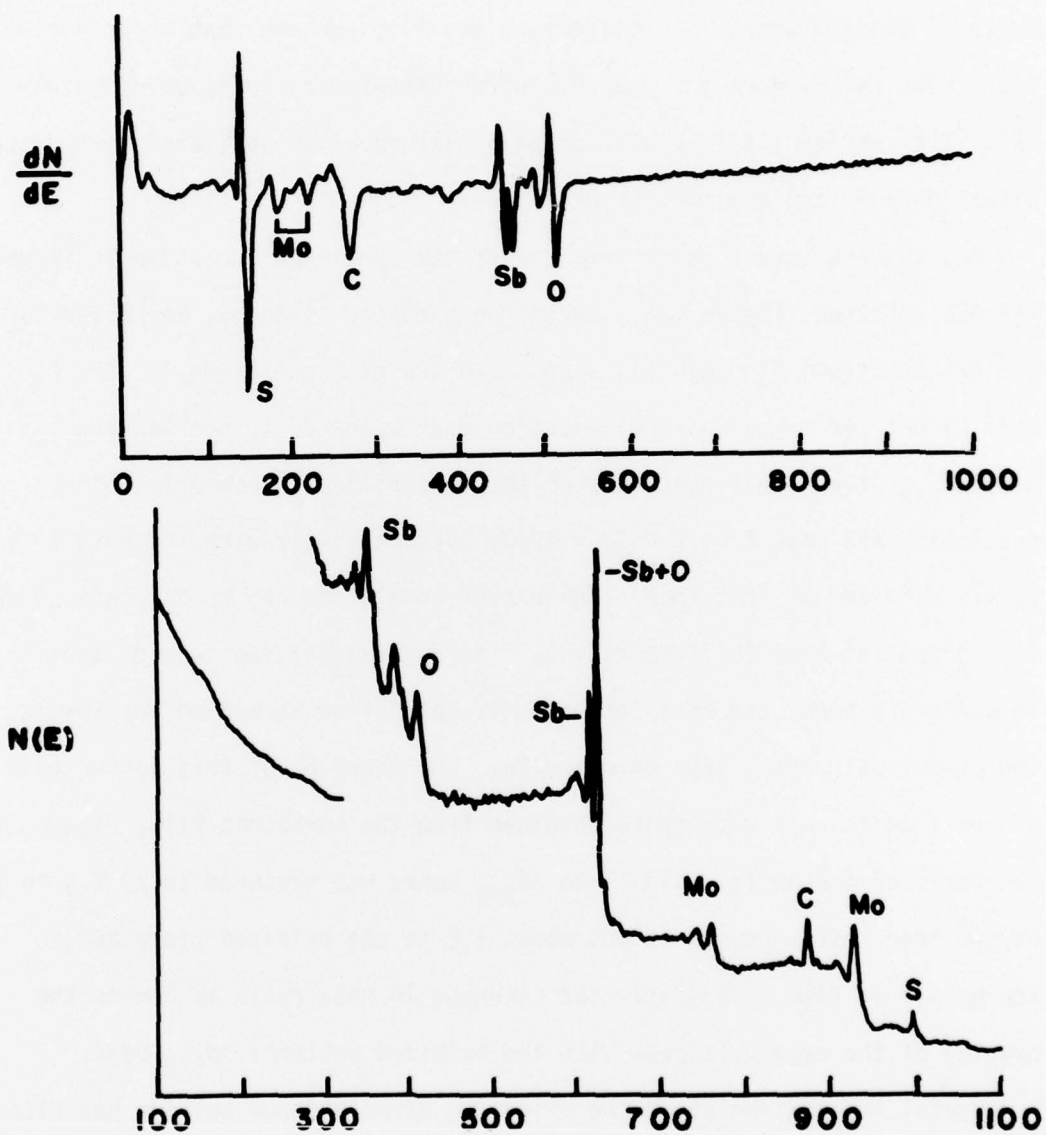FIGURE 16 - Analysis of co-sputtered MoS$_2$ and Sb$_2$O$_3$ using (a) Auger electron spectroscopy, and (b) X-ray photo-electron spectroscopy.

34
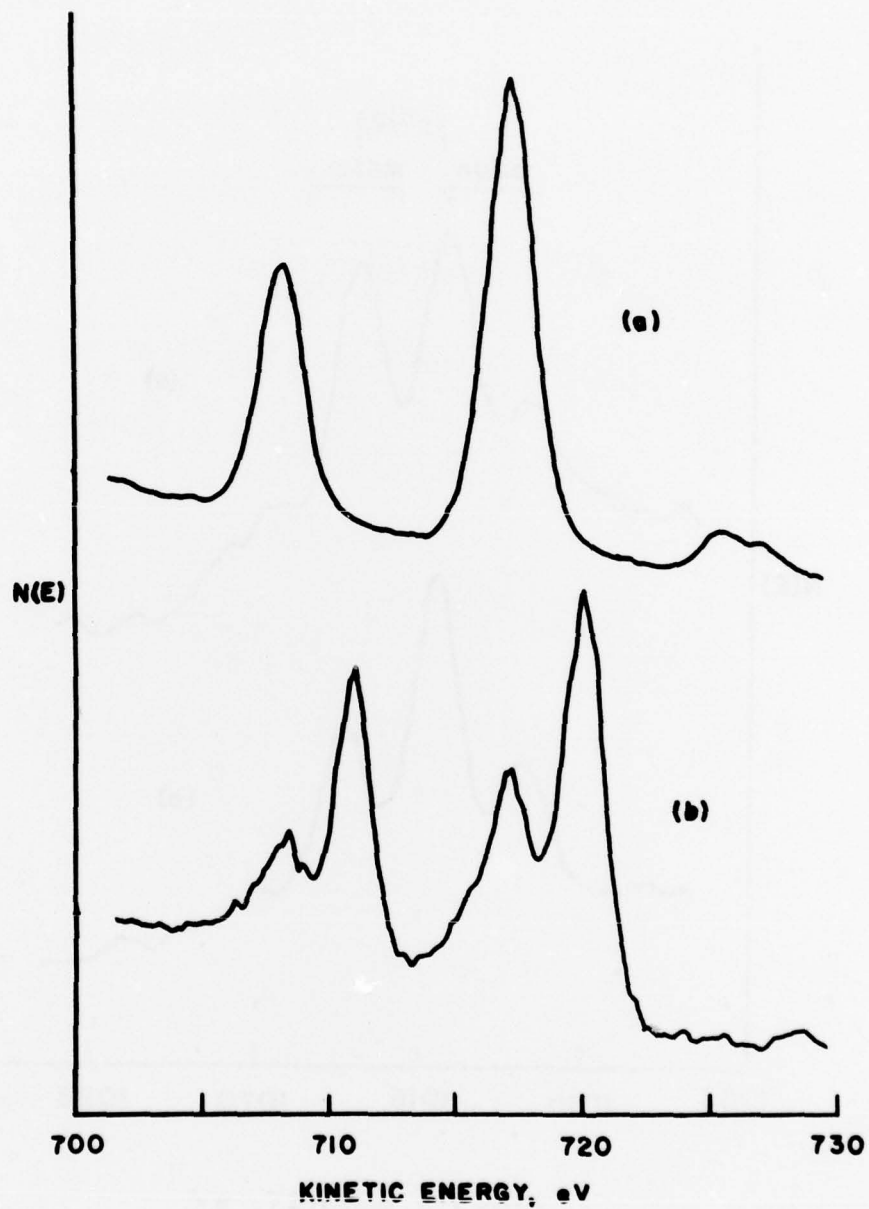
FIGURE 17 - XPS spectra from, (a) MoS_2 + Sb_2O_3 burnished film, and (b) partly oxidized InSb. Spectrometer resolution was 1 eV.
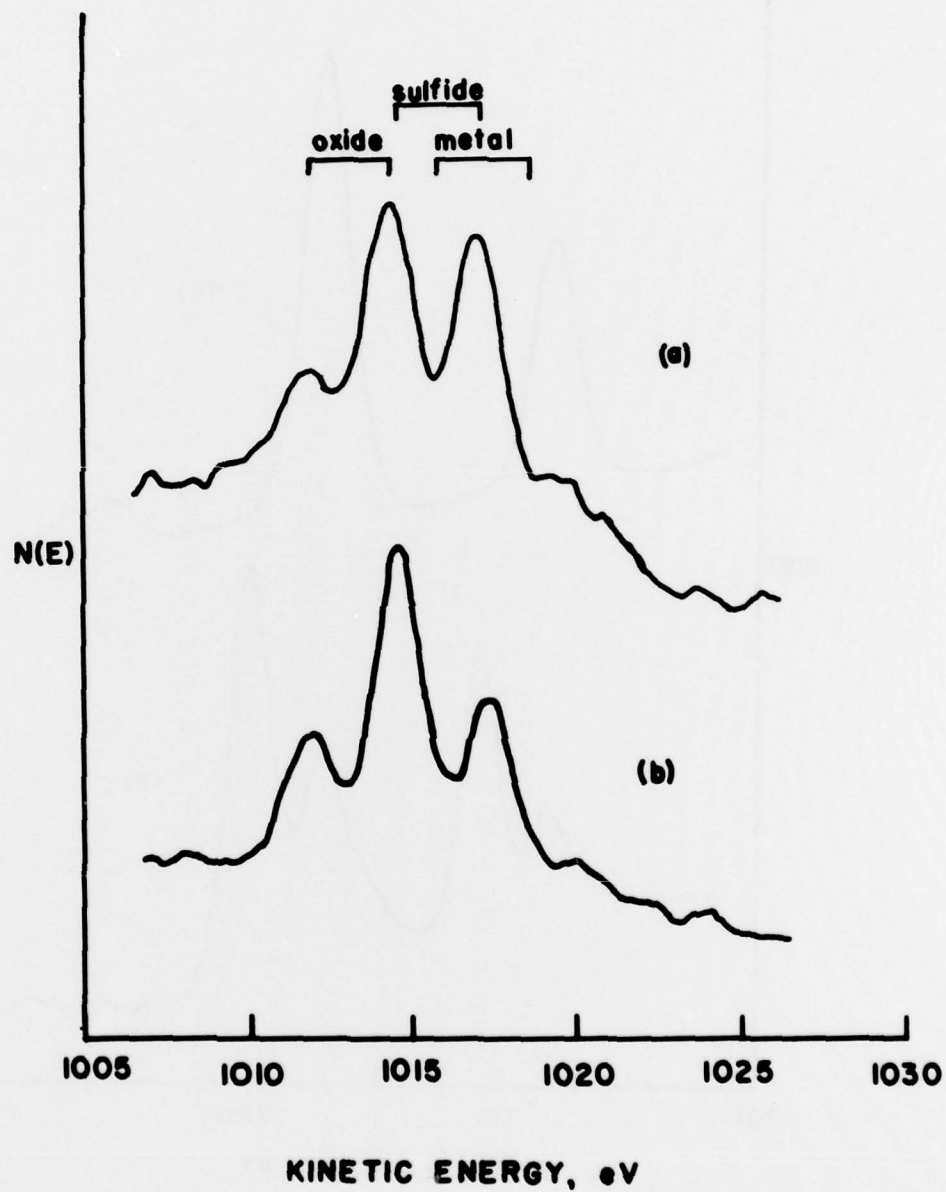
FIGURE 18 - Molybdenum 3d XPS spectra from two partly worn gas
bearings, (a) and (b).   Spectrometer resolution was
1 eV.

spectrum is a doublet so different molybdenum chemical states(at least two) are present on the partly worn bearings. Molybdenum 3d reference spectra were obtained and are shown in Figure 19, (a) being from (air) oxidized molybdenum, (b) from a burnished molybdenum disulfide film and (c) from clean molybdenum. The positions of these reference spectra are also shown in Figure 18. Identification of the two main chemical states of molybdenum on the bearings is now quite clear, a mixture of molybdenum oxide and molybdenum disulfide. Note that the bearing in Figure 18(b) is more oxidized than that in Figure 18(a).

FIGURE 19 - Molybdenum 3d XPS spectra from, (a) air oxidized
molybdenum, (b) burnished MoS_2 film, and (c) clean
molybdenum. Spectrometer resolutions was 1 eV.

SECTION VI

OTHER SURFACE STUDIES

1.   ELECTRON BOMBARDMENT OF BORON NITRIDE

A study was undertaken to investigate possible changes in surface
composition and chemistry during electron bombardment of boron nitride
(BN). Two types of BN were analyzed - isotropic BN and anisotropic BN.
BN is used as an insulating material in traveling wave tubes (TWT) and if
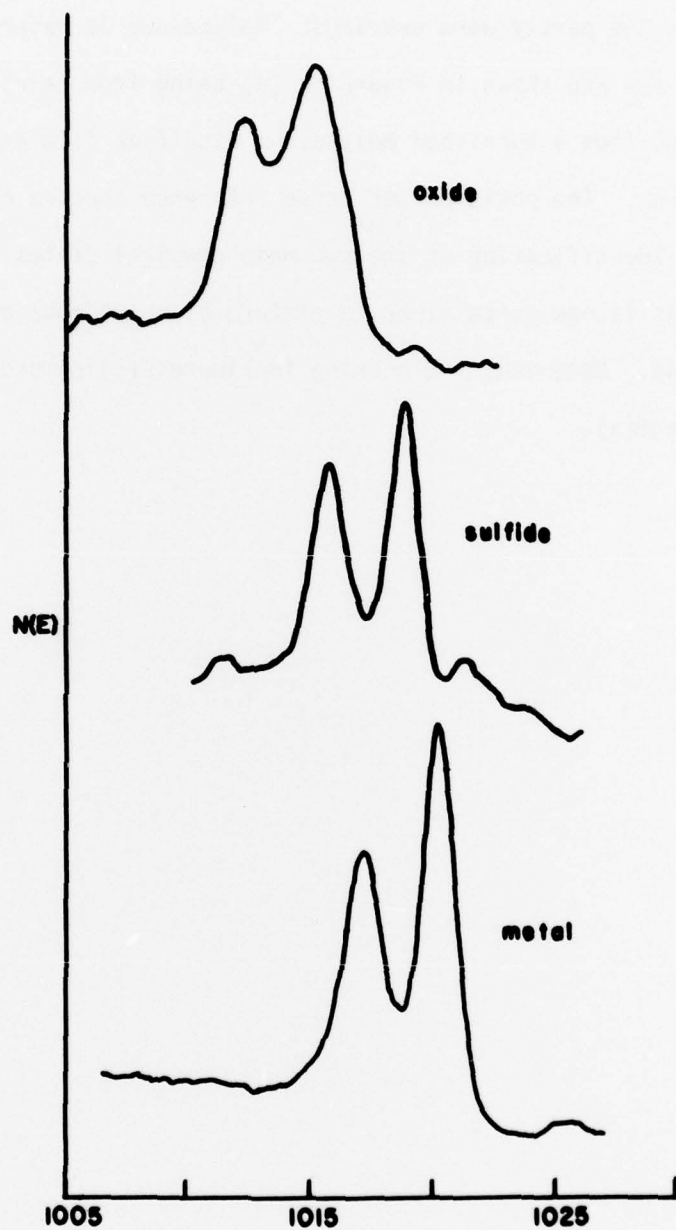degradation of BN occurred under electron bombardment it could lead to
premature failure of TWT's.

Both AES and XPS measurements were made before and after bombard-
ment. Electron bombardment was carried out with a 30μA, 5kV electron
beam having a beam diameter of about 1mm. Under such conditions many
compounds suffer surface decomposition, but no such decomposition was
observed for BN. Reference AES and XPS spectra of boron were also taken
and it was quite apparent that if significant decomposition occurred it
would have been detected. The level of detectability for a change in sur-
face composition or chemistry of BN is estimated to be about 10%. The
only change noted was an increase in the surface carbon concentration
with bombardment time, due to electron beam cracking of carbon contain-
ing gases in the vacuum chamber on the BN. (The background pressure
was about $2x10^{-8}$ Pa during bombardment).

2.   SMUT ON STAINLESS STEEL SURFACES

Smut is a loosely adhering material that forms on materials such
as Al, Ti, their alloys, and stainless steel during chemical treatment.

39

Smut has been shown to decrease initial bondability and probably decreases effective service lifetime. It had been assumed by some workers that smut on their samples was due to graphite. The low carbon content and the availability of numerous known smutting materials including large amounts of Cu and Si, make it unlikely that smut on stainless steel consists only of graphite. AES and XPS measurements of smutted stainless steel surfaces showed the presence of Si and Cu on these surfaces in much larger amounts than on desmutted surfaces. The silicon found was in the form of silicon dioxide. From such studies of smut formation it may be possible to modify processes to eliminate it.

3.   STRIPPABLE OXIDE FILMS

It is possible to use an anodization process that permits the oxide film to be stripped from a number of materials. This process may be of use in several technologies where fresh "super clean" surfaces are needed. On the other hand, such a surface is very undesirable for adhesive bonding, but it does serve as a model for interfacial failure to try to determine what bearing the chemistry at the interface has to do with adhesion. AES and XPS studies were made on Ta samples and F was found to be present on both the metal and oxide surfaces. Typical AES and XPS spectra from the stripped metal are shown in Figures 20 (a) and (b) respectively. It is planned to study specimens excluding or modifying F to determine the effect on adhesion.

4.   ANALYSIS OF ANGLE OF ATTACK TRANSMITTER

AES analysis of components of an F-4 angle of attack transmitter were made to determine the presence of $NbSe_2$ lubricant on parts. $NbSe_2$
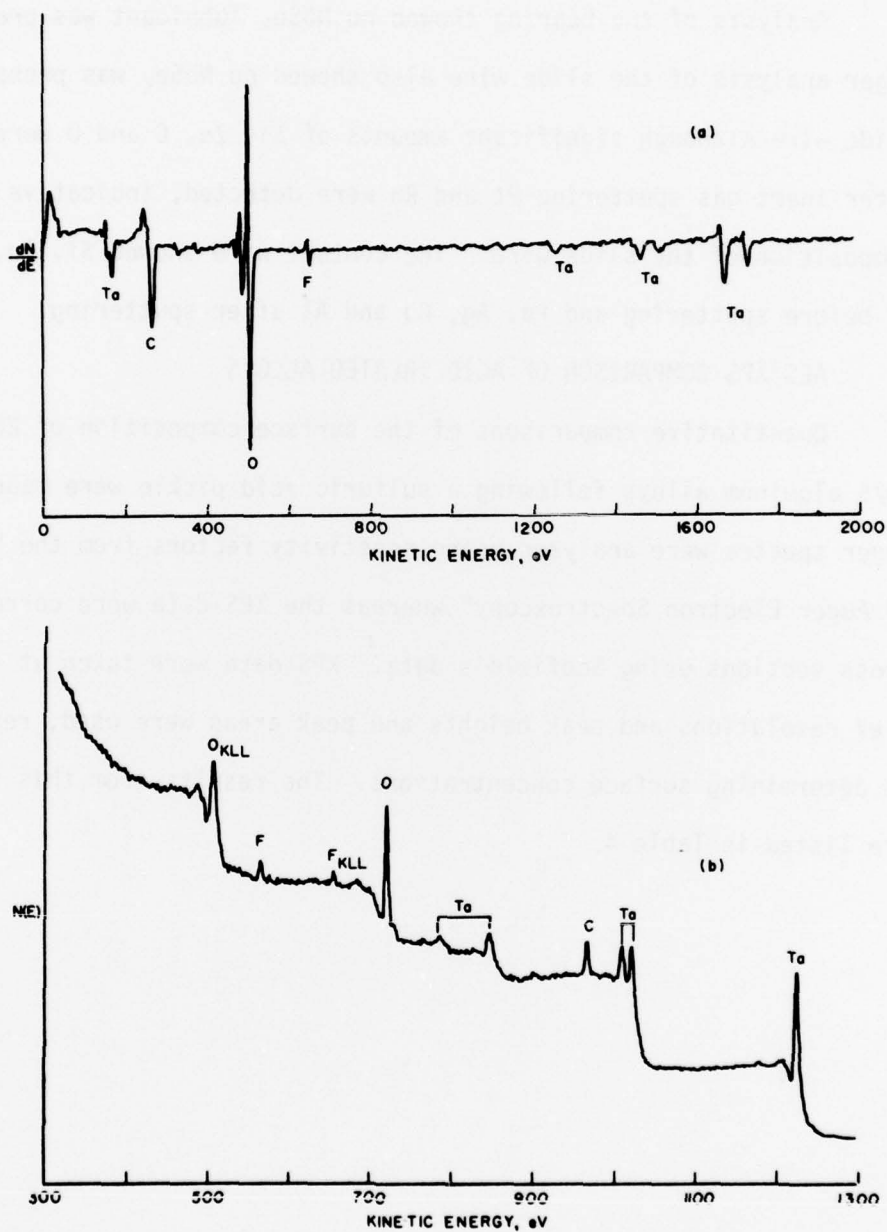
FIGURE 20 - Analysis of Ta after stripping its oxide, (a) using
Auger electron spectrocopy, and (b) using X-ray photo-
electron spectroscopy.

41

was used as a lubricant for the slide wire in the transmitter and it was thought that some $NbSe_2$ may have reached the bearings in the transmitter.

Analysis of the bearing showed no $NbSe_2$ lubricant was present. Auger analysis of the slide wire also showed no $NbSe_2$ was present on the slide wire although significant amounts of Si, Zn, C and O were found. After inert gas sputtering Pt and Rh were detected, indicative of the composition of the slide wire. The contact wire showed Si, Zn, N and Cl before sputtering and Pd, Ag, Cu and Al after sputtering.

5.   AES/XPS COMPARISON OF ACID TREATED ALLOYS

Quantitative comparisons of the surface composition of 2024 and 7075 aluminum alloys following a sulfuric acid pickle were made. Auger spectra were analyzed using senstivity factors from the "Handbook of Auger Electron Spectroscopy" whereas the XPS data were corrected for cross sections using Scofield's data.[1] XPS data were taken at 4 eV and 1 eV resolutions and peak heights and peak areas were used, respectively, in determining surface concentrations. The results from this study are listed in Table 4.

TABLE 4

RELATIVE SURFACE CONCENTRATIONS OF ELEMENTS FROM A 7075
ALUMINUM ALLOY OBTAINED FROM AES AND XPS

RELATIVE CONCENTRATIONS

ELEMENTS	AES (PEAK-TO-PEAK HEIGHTS)	XPS (PEAK HEIGHTS)	XPS (PEAK AREAS)
Si	2.8	--	--
P	3.4	7.0	--
S	0.49	3.5	--
C	9.0	43	53
Ca	4.5	--	--
N	1.1	8.7	--
O	100	100	100
Cu	2.5	8.3	3.4
Zn	2.6	1.4	1.4
Mg	2.6	--	--
Al	68	43	55

APPENDIX

f. Deconvolution Program for XPS Data

```
 10=        PROGRAM DECON(INPUT,OUTPUT,TAPE 1=OUTPUT,TAPE 2=INPUT,TAPE 3
 20=        1,TAPE 4,TAPE 6)
 30=        DIMENSION F(1000),G(1400),H(1000),X(1000),Y(1000),CH(1000)
 40=        CHECK=1.0
 50=        WRITE 10
 60=10      FORMAT(/,* NUMBER OF DATA POINTS...*)
 70=        READ*,N
 80=        DO 20 I=1,1400
 90         G(I)=0.0
100=20      CONTINUE
110=        READ (3,30) (CH(I),H(I),I=1,N)
120=30      FORMAT (2F13.6)
130=        DO 50 I=1,N
140=        X(I)=H(I)
150=50      CONTINUE
160=        READ (6,40) (G(I),I=351,1050)
170=40      FORMAT (F13.6)
180=        WRITE 60
190=60      FORMAT (/,*WIDTH OF DECONVOLUTION REGION IS 2L+1' ENTER L...*)
200=        READ*,L
210=        IMIN=1+L
220=        IMAX=N-L
230=190     CONTINUE
240=        WRITE 80
250=80      FORMAT(/,* ENTER NUMBER OF APPROXIMATIONS TO BE MADE...*)
260=        READ*,KMAX
270=        DO 90 K=1,KMAX
280=        DO 310 I=1,N
290=        Y(I)=0.0
300=310     CONTINUE
310=        DO 100 I=IMIN, IMAX
```

45

```
320=       JMIN=I-L
330=       JMAX=I+L
340=       DO 110 J=JMIN,JMAX
350=       ISUB=700+J-I
360=       Y(I)=X(J)*G(ISUB)+Y(I)
370=110    CONTINUE
380=100    CONTINUE
390=       DO 320 I=IMIN,IMAX
400=       IF (Y(I).LT.0.0) CHECK=10.0
410=       IF (CHECK-10.0) 320,330
420=330    WRITE (1,340) I
430=340    FORMAT(/,1X,*Y(I) LESS THAN 0*, 5X,I3)
440=       GO TO 180
450=320    CONTINUE
460=349    FORMAT(5X,F13.6,5X,F13.6)
470=       DO 120 I=IMIN,IMAX
480=       X(I)=X(I)*H(I)/Y(I)
490=120    CONTINUE
500=90     CONTINUE
510=       WRITE 170
520=170    FORMAT(/,*TOTAL NO. OF APPROX. TO BE MADE...*)
530=       READ*,MAX
540=       IF (MAX-KMAX) 190,180
550=180    CONTINUE
560=       WRITE (4,230) (CH(I),X(I),I=IMIN,IMAX)
570=230    FORMAT(2F13.6)
580=       NX=IMAX-IMIN+1
590=       WRITE (1,240) NX
600=240    FORMAT(1X,I3,* DATA POINTS TO BE PLOTTED ARE ON TAPE4*)
610=350    END
```

REFERENCES

1. J. H. Scofield, J. Electron Spectrosc. Relat. Phenom., Vol. 8, pp. 129 (1976).

2. K. A. G. MacNeil and R. N. Dixon, J. Electron Spectrosc. Relat. Phenom., Vol. 11, pp. 315 (1977).

3. N. Beathan and A. F. Orchard, J. Electron Spectrosc. Relat. Phenom., Vol. 9, pp. 129 (1977).